Electronic Supplementary Material (ESI) for Lab on a Chip

Lab on a Chip

Supplementary Information

Title: Microwave sensing and heating over individual droplets in microfluidic devices

Authors: Muhammed S. Boybay, Austin Jiao, Tomasz Glawdel and Carolyn L. Ren

S1. Resonator Design

The resonator structure consists of a circular loop with a small capacitive gap and is designed to efficiently confine microwave energy into a small volume. Energy within the resonator is mostly dissipated as conductive loss along the loop and as dielectric loss within the capacitive region. At the resonance frequency, energy is transmitted into the capacitive region and any material in the gap experiences dielectric heating.

i. Inductance and capacitance of the resonator

Circulation of current around the resonator loop generates inductance while the gap region generates capacitance. As a result the loop resonates at the following frequency:

$$f = \frac{1}{2\pi\sqrt{LC}} \tag{S1}$$

In our design, the loop has a radius of 3.75 mm and the capacitive gap has a separation of 20 μm (see Figure S1 for details). The loop without any substrate resonates at 5.759 GHz. To calculate the inherent inductance and capacitance of the loop, the capacitive gap is replaced by a sheet with a defined capacitance, as the capacitance of the gap is unknown. The resonance of the new structure becomes:

$$f = \frac{1}{2\pi\sqrt{L(C_1 + C_2)}} \tag{S2}$$

where C_1 is the value of the added lumped capacitance and C_2 is the remaining capacitance between the arms. Therefore Eq. (S2) can be written as:

$$LC_1 + LC_2 = \frac{1}{4\pi^2 f^2} \tag{S3}$$

Eigenvalue solutions of the structure are obtained using Ansoft HFSS. The plot as a function of C_1 allows the value of L to be extracted which is the slope of the graph as shown in Figure S2. Two different sizes

of the capacitance sheet are used to verify the method. The average inductance is found to be 21.149 nH. Knowing that the resonance frequency is equal to 5.759 GHz, the capacitance is calculated as 36.112 fF.

The resonator with T shaped capacitance The resonator with lumped capacitance

Figure S1: The capacitive junction is replaced by a lumped capacitance to obtain the capacitance and inductance values of the resonator. Two different sizes for the replaced section are used to verify the accuracy of the method.

ii. Excitation of the resonator and energy confinement

The resonator is excited by inductive coupling using a concentrically aligned excitation loop around the resonator. The separation between the excitation loop and resonator, as well as the trace width of the excitation loop, were optimized to obtain the most efficient energy coupling using Ansoft HFSS. The optimum excitation loop design has a radius of 6.45 mm and a trace width of 1 mm. According to simulations, the resulting system is able to deposit 45% of the incident power in to a 2 nl water droplet placed within the capacitive gap.

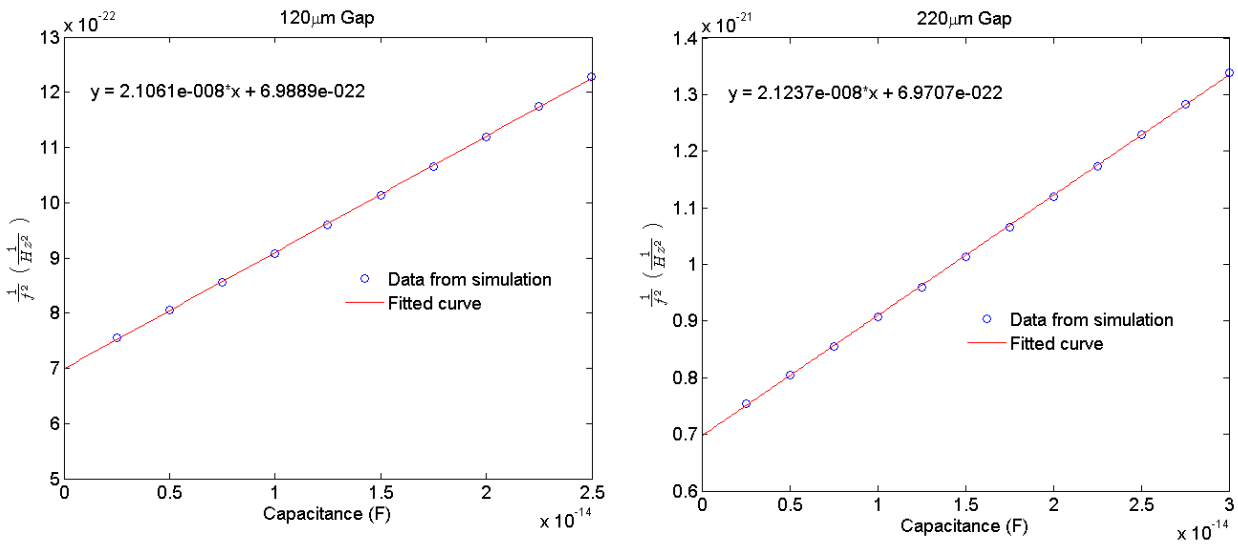

(a) (b)

Figure S2: The inductance of the resonator is extracted by adding a lumped capacitance to the gap of the resonator. The inductance is equal to the slope of the lines. The error between two numerical experiments is 0.8%.

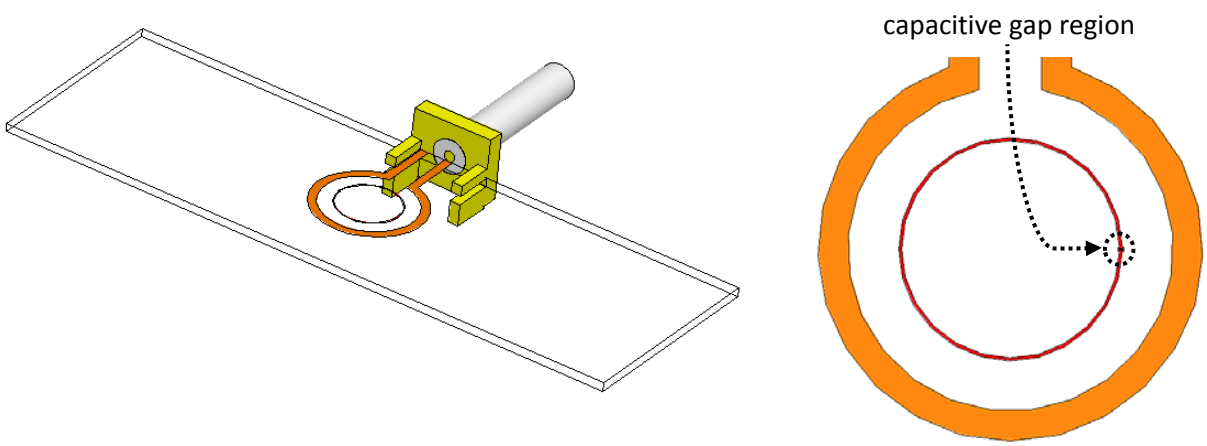

Figure S3: The structure used in the simulation for optimizing the excitation.

iii. Resonance modes of the resonator

The resonator can serve as a sensor and/or a dielectric heater. When used for resonance frequency measurements, the structure is connected to a vector network analyzer (VNA) using an SMA connector and a coaxial line while for heating purposes it is connected to a RF signal generator, as shown in Figure S4. Then the VNA and the RF signal generator are connected to a computer for controlling purposes.

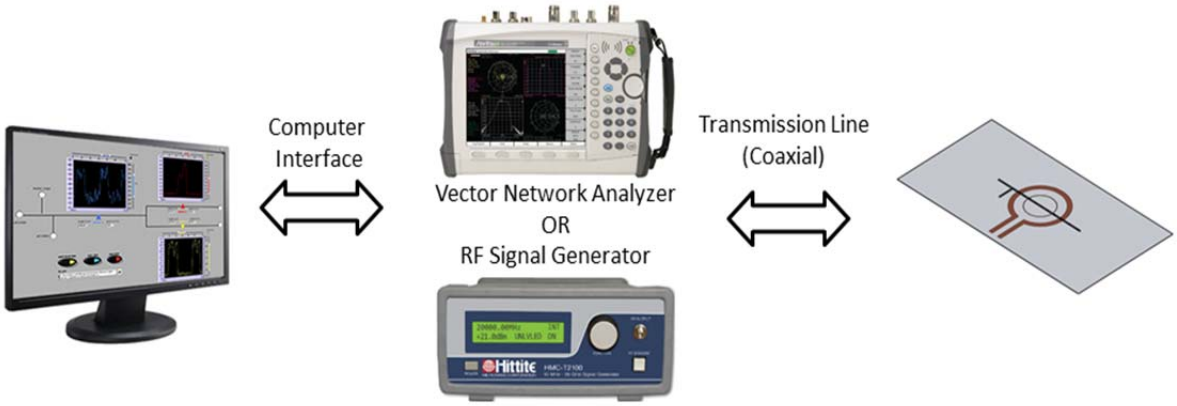

Figure S4: Description of the setup for microwave system.

The confinement of the electric field increases the sensitivity of the resonator when employed as a sensor and the heating efficiency when used as a heater. To present the energy confinement and the difference between the resonance modes, eigenvalue solutions of the structure were obtained using Ansoft HFSS and presented in Figure S5. It can be seen that when the resonator is electrically small, the electric field is efficiently confined to the capacitive region. On the modes with higher resonance frequencies, confinement is degraded.

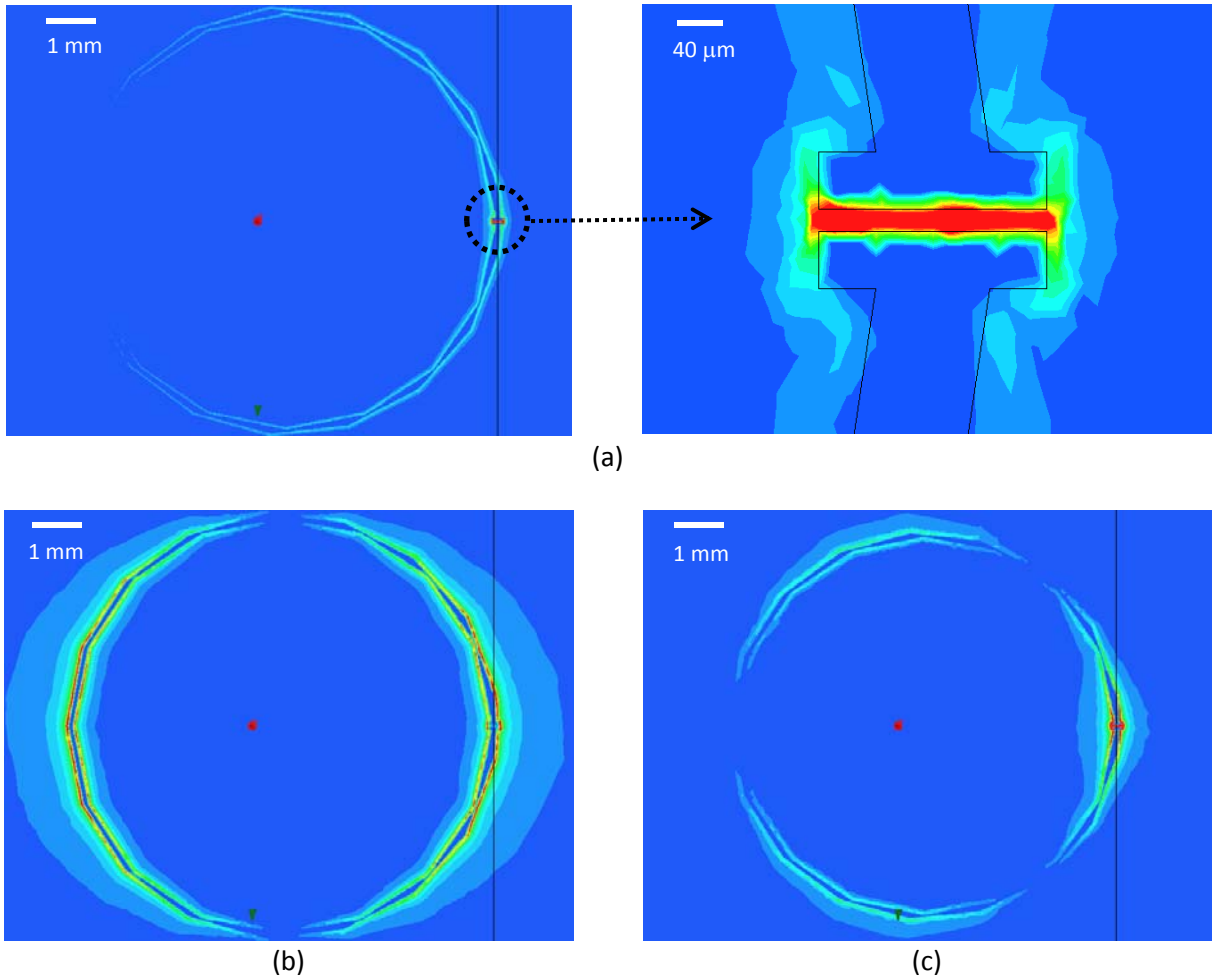

Figure S5: Electric field distribution of the first three modes of the resonator, (a) 5.78 GHz, (b) 9.83 GHz, (c) 10.44 GHz.

S2. Chip Fabrication

i. Fabrication of Microwave Components

Conductive losses must be minimized to maximize the performance of electrically small resonators. For this reason, the thickness of any microwave component must be larger than the skin depth of the material. For copper, the skin depth at 2 GHz corresponds to 1.5 µm. Therefore we developed a method to fabricate glass substrates containing microwave components made of copper with a thickness larger

than 5 μm, as illustrated in Figure S6. Using this method, we are able to fabricate structures with lateral features as small as 10 μm (see Figure S7).

Briefly, glass slides that have a 50 nm thick copper film deposited on one side (CU134, EMF-Corp.) are spin-coated at 1500 RPM for 60 seconds with S1813 photoresist (Rohm and Haas). A soft bake is then performed at 120°C for 75 s. Microwave component details are patterned by UV lithography and then developed using MF-319. The copper slide is then placed into an electroplating solution of 0.2 mol L^{-1} copper sulphate pentahydrate, 0.1 mol L^{-1} of boric acid, and 0.1 mol L^{-1} of sulphuric acid. Copper is deposited onto the surface of the copper slide at 2 mA for 4 mins and then at 10 mA for another 20 mins. After electroplating, the slide is retrieved from the solution and the photoresist is removed using acetone. The thin bottom layer of copper is etched off using a diluted solution of 5% ferric chloride in water yielding around 8 μm thick copper traces. Subsequently, the microwave traces are passivated by spincoating a thin layer of hard PDMS (Dow Corning) at 4000 RPM for 60 s. Hard PDMS is used because of its stability to rapid temperature changes. Finally, SMA connectors are soldered onto the excitation loop of the microwave components afterwards.

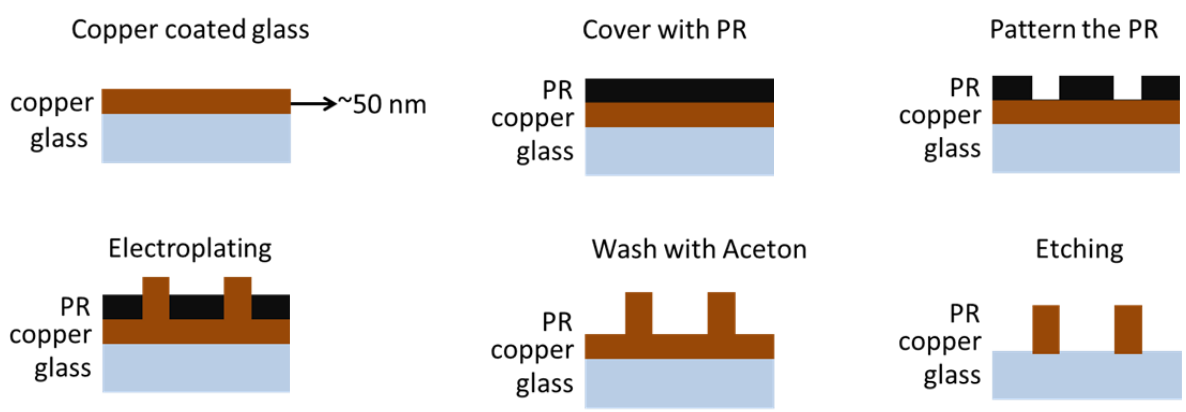

Figure S6: Steps for fabrication microwave components on glass substrates

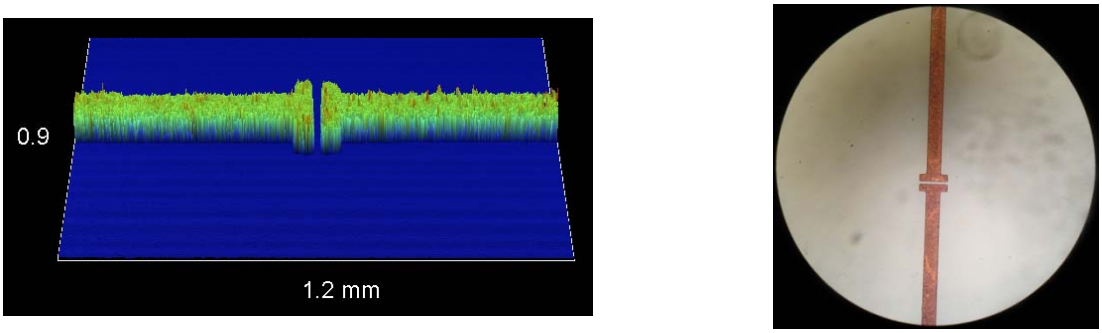

(a) (b)

Figure S7: **a,** The thickness of the microwave components were measured using optical profilometer. **b,** The image of the fabricated microwave components

ii. Microfluidic Chip Fabrication

Standard soft lithography techniques were used to fabricate micro channels. Masters made of SU8 photoresist are first fabricated on Si wafers and then PDMS mixture is poured onto the master and cured at 190 °C for about 2 hrs. The fabricated microfluidic chips and the glass substrates with microwave components are bonded using oxygen plasma at 29.7 W, 500 mTorr for 45 s using a microscope for alignment. For the chips that are used for droplet generation, the channels are treated with fluorinated surface treatment (aquapel) for 2 mins and then purged with air. The treatment is completed by leaving the chips in air for 30 mins. The fabricated channels are 200 μm wide and 50 μm high. The structures of the channels for droplet generation are presented in Figure S8.

(a) (b)

Figure S8: **a,** The microfluidic chip used for droplet heating and sensing. **b,** The microfluidic chip used for mixing analysis.

S3. Thermally Induced Manipulation of Droplets:

We anticipate heat generation to be concentrated within the small resonator gap which would lead to large temperature gradients within the droplet. To test this hypothesis we applied the microwave heater to enhance mixing within droplets. It has been observed that when droplets are transported through a straight microchannel viscous stresses generate two symmetric vortices in each half of the droplet . Mixing between the two halves of the droplet occurs due to cross-diffusion, which is a slow process. By creating thermally induced cross-stream marangoni stresses we anticipated that mixing could be enhanced.

In order to perform such an experiment, heterogeneous droplets were generated with one half containing a fluorescent dye (see Figure S10). Several resonator conditions were tested by altering the orientation of the resonator gap with the microchannel (0, 45, 90), and changing the gap structure (spiral, zig-zag, ect.) and flow conditions (high speed, low speed, with surfactants and without). However, in all cases we did not observe a significant amount of mixing when the droplet passed through the heating zone (see Figure S10). Similarly, we were unable to manipulate the droplets (stop or deflect them) with the current heater design. These results suggest that temperature gradients are not severe and heat up of the droplet is uniform.

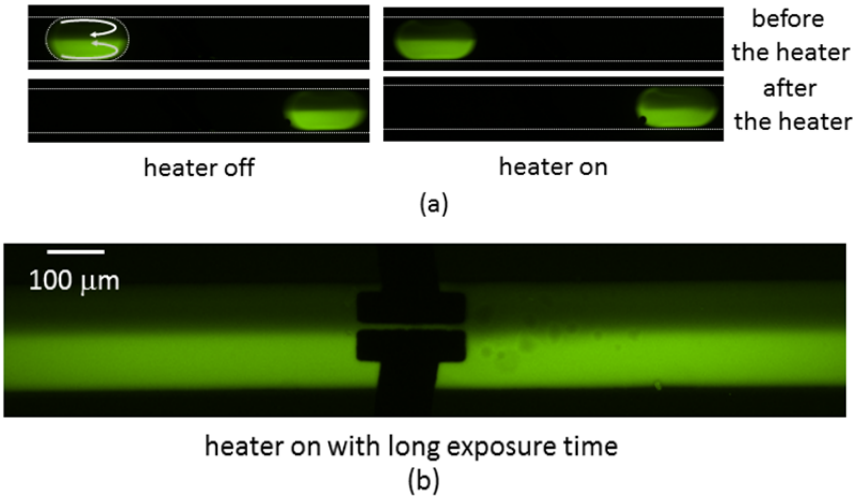

Figure S9: **a**, Investigation of any mixing effect as a result of the heating was conducted by generating droplets with heterogeneous content. Half of the droplet was filled by dyed water (lower half) and the other half was filled with pure water (upper half). The vortices within the droplet cannot mix these two halves. The only mixing occurs as a result of diffusion. The small amount of emission obtained from the upper halves are as a result of the diffusion and the mixing occurred during the generation of the droplets (see supplementary file for more detail). Singe droplet images show that the heating is not localized to initiate mixing as a result of marangoni stresses. **b**, In order to quantify any possible mixing effect, the exposure time was increased to generate images that look like a single phase flow. These images also show that there is no significant mixing with droplets due to the heating.

References

[1] D. Malsch, M. Kielpinski, R. Merthan, J. Albert, G. Mayer, J. M. Kohler, H. Sube, M. Stahl and T. Henkel, "mPIV-Analysis of Taylor flow in micro channels," *Chemical Engineering Journal,* vol. 135S, pp. S166-S172, 2008.